obtained by the FEM is also included in Tables 1 and 2. Noted that for the values of α considered in this Note, for $\alpha = 0.0$, 0.1, and 1.0, Eq. (6) gives an underestimate. For $\alpha = 10.0$, 100.0, and for $\alpha \to \infty$, Eq. (6) gives an overestimate for the stressed frequency. This is due to the effect of the variation of the mode shapes changing from the simply supported case to the clamped case. The results are presented in this Note are for the two typical values of $\alpha = 1.0$ and 100.0 only. It can be seen from Tables 1 and 2 that the present results are in good agreement with the finite element results with the initial stress parameter $\bar{\lambda}$ up to 0.6; the error is less than 3.5%. However for higher values of $\bar{\lambda}$, for example, 0.8, the results differ by about 5–12%, depending on the values of α and $\bar{d}$. The results for $\alpha = 0.0$ (simply supported tapered beam), 0.1, 10.0, 1000.0 and $\alpha \to \infty$ (clamped tapered beam) are also computed, but not given here for the sake of brevity, and show the same trend. This is because the eigenvectors for higher values of $\bar{\lambda}$ are not exactly the same, violating the assumption made in the present analysis. However, for all practical purposes the present results are good enough and can be used effectively and quickly by design engineers to assess the fundamental frequency parameter of initially stressed beams with end rotational restraints.

Conclusions

A simple formula is proposed to predict the fundamental frequency of initially stressed tapered beams with end elastic rotational restraints for a given initial stress by knowing its stress free frequency. Because fundamental frequency is one of the important design parameters during the design phase of any structural element, a quick method of its estimation with minimum computational effort is very useful for designers. The proposed formula is expected to meet this requirement. Numerical results presented for typical tapered beams with end elastic rotational restraints demonstrate its applicability. These results are found to be in reasonably good agreement with those obtained from the FEM and, hence, can be effectively used during the design phase.

References

[1]Shastry, B. P., and Venkateswara Rao, G., "Initially Stressed Vibrations of Beams with Two Symmetrically Placed Intermediate Supports," *Journal of Sound and Vibration*, Vol. 103, No. 4, 1985, pp. 593–595.

[2]Kanaka Raju, K., and Venkateswara Rao, G., "Free Vibration Behaviour of Prestressed Beams," *Journal of Structural Engineering*, Vol. 112, No. 2, 1986, pp. 433–437.

[3]Singaravelu, J., Singh, G., and Venkateswara Rao, G., "Free Flexural Vibrations of Initially Stresses Tapered Beams Including the Effects of Shear Deformation and Rotary Inertia," *Journal of Sound and Vibration*, Vol. 158, No. 3, 1992, pp. 572–575.

[4]Shastry, B. P., and Venkateswara Rao, G., "Vibrations of Partially Stressed Beams," *Journal of Vibration, Acoustics, Stress and Reliability in Design*, Vol. 108, No. 4, 1986, pp. 474–475.

[5]Kanaka Raju, K., and Venkateswara Rao, G., "Vibration Behaviour of Tapered Beams Columns," *Journal of Engineering Mechanics*, Vol. 114, No. 5, 1988, pp. 889–892.

[6]Lee, Y. S., and Ke, H. Y., "Free Vibrations of a Non-Uniform Beam with General Elastically Restrained Boundary Condition," *Journal of Sound and Vibration*, Vol. 136, No. 3, 1990, pp. 425–437.

[7]Gutierrez, R. H., Laura, P. A. A., and Rossi, R. E., "Natural Frequencies of a Timoshenko Beam of Non-Uniform Con-Section Elastically Restrained at Core End and Guided at the Other," *Journal of Sound and Vibration*, Vol. 141, No. 1, 1990, pp. 174–189.

[8]Maurizi, M. J., Bambill De Rossit, D. V., and Laura, P. V. V., "Free and Forced Vibrations of Beams Elastically Restrained Against Translation and Rotation at the Ends," *Journal of Sound and Vibration*, Vol. 120, No. 3, 1988, pp. 626–630.

[9]Sato, K., "Transverse Vibrations of Linearly Tapered Beams with Ends Rotational Elastically Against Rotation Subjected to Axial Force," *International Journal of Mechanical Sciences*, Vol. 22, No. 2, 1980, pp. 109–115.

[10]Venkateswara Rao, G., Rajasekhara Naidu, N., "Free Vibration and Stability Behaviour of Uniform Beams and Columns with Nonlinear Elastic End Rotational Restraints," *Journal of Sound and Vibration*, Vol. 176, No. 1, 1994, pp. 130–135.

[11]Zienkiewicz, O. C., *The Finite Element Method*, McGraw–Hill, London, 1977.

A. Berman
Associate Editor

Visualization Study of a Passively Perturbed Swirling Jet

T. Terry Ng*
University of Toledo, Toledo, Ohio 43606

I. Introduction

THE effect of flow disturbances on jet development is a phenomenon of major practical significance. In addition to the instabilities governing the spanwise vortex development, the computational study by Pierrehumber and Widnall[1] identifies a broadband fundamental mode instability that leads to a streamwise vorticity concentration. A number of studies in recent years have also been focused on forcing other instabilities such as the low-level azimuthal modes and on controlling the jet flow by alterations of the nozzle geometry. Two examples of these studies are Long and Petersen[2] and Longmire et al.[3]

Recent advances in actuator technology allowed an elaborate control scheme by Davis and Glezer.[4] In this scheme an azimuthal array of nine synthetic jet actuators was placed around the circumference of a round jet exit. The control was used to manipulate both mixing at the small scale and entrainment at the large scale. Many modes of jet flow could be induced. Additionally to jets consisting of mostly axial flow, there have also been many investigations on jets with swirl. A recent example is that of Wicker and Eaton,[5] where streamwise vorticity with an opposite sign to the main swirl was injected using four vortex generators placed evenly deep inside a nozzle. A four-lobed structure was subsequently observed in the jet.

In this investigation the effects of small, discrete perturbations around the perimeter of a jet with and without swirl are studied. The main objective of present effort is to establish a relationship between the number of perturbations and the resulting flow structure. The work is mostly qualitative, with flow visualization being the main tool.

II. Experimental Setup

The experiment was conducted in a jet flow apparatus consisting of a 25-mm-diam, 60-mm-long nozzle attached to a 14-cm-diam stagnation chamber. Screens, perforated plates, and flow straighteners are positioned inside the stagnation chamber and upstream of a single 5-cm diam side entrance, which provides the swirling component.

Five different jet exit geometries, each with a nominal diameter of 2.22 cm and length of 24 mm, were tested. The baseline geometry is circular and is designated N-00. Other jet exits, shown in Fig. 1, are designated N-02, N-03, N-04, and N-08 with the numeral indicating the number of perturbations. Perturbations on the N-02, N-03, and N-08 exits are in the form of small, circular-arc notches at the exit circumference. The notches are approximately 7.0 mm in width and 1.5 mm in depth. Merging every two notches on the N-08 geometry formed the N-04 exit.

The experiment was conducted at a Reynolds number of approximately 1.8×10^4 based on the nominal exit diameter and the main (nonswirling) flow. The exit flow characteristics were quantified using a single hot-wire probe. Results for all of the exit geometries indicate a uniform exit velocity profile with an exit boundary-layer thickness of about 1 mm and an initial turbulent level of 0.4%.

For convenience the main flow is held fixed. The ratio of side-to-main volumetric flow is about 0.25. Although the addition of side flow increases the Reynolds number, qualitatively and visually the development of the jet did not seem particularly sensitive to moderate variations in the overall flow rate. The smoke for flow visualization was generated using a Rosco fog machine, with either a strobe light or laser sheet providing the illumination. Images were

Received 3 April 2000; revision received 3 August 2000; accepted for publication 18 August 2000.

*Professor, Department of Mechanical Engineering.

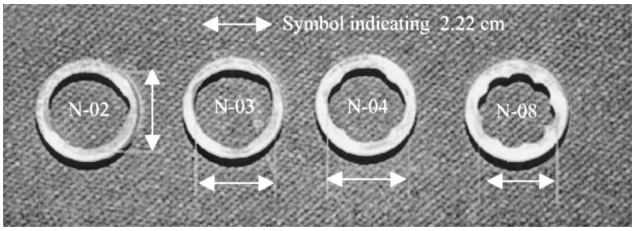

Fig. 1 Nozzle exit geometries.

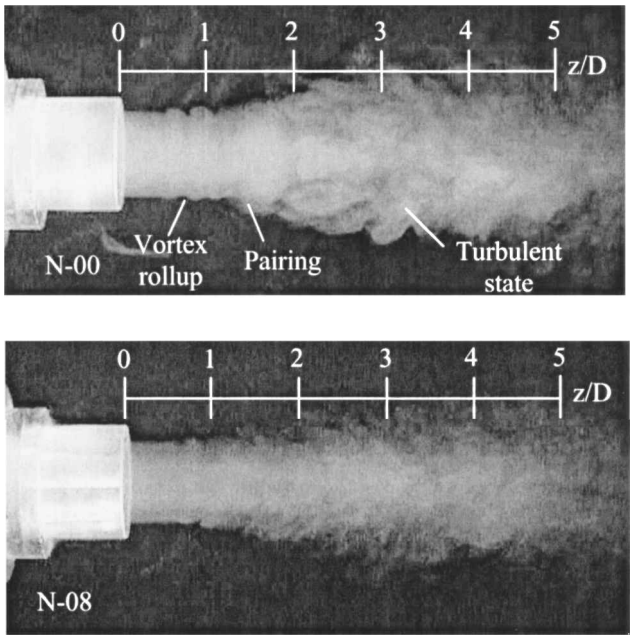

Fig. 2 Comparison of N-00 and N-08 jets without swirl: strobe light and smoke.

recorded using a digital video camera and transferred later to a computer for processing.

III. Results

Figure 2 shows the flow images, captured using a strobe light, of N-00 and N-08 jets without swirl. By manipulating the frequency of the strobe, the N-00 jet can be observed to display the typical initial vortex roll up, pairing, and formation of three-dimensional structures. The transformation into a turbulent jet begins at z/D of about two. The N-08 results show a rather different near-field development. No axisymmetrical vortex roll up or pairing was observed using either the strobe light or laser sheet. Instead, the periodic perturbations led to the formation of relatively steady, streamwise structures in the shear layer that visually appear as striations along the outer surface of the jet. Compared to the circular jet, the growth rate of the N-08 jet appears to be reduced for the first two to three diameters.

Figure 3 shows selective laser-sheet visualization of the N-08 jet. Without swirl the perturbations impose controlled wrinkles in the shear layer, which rapidly evolve into eight pairs of counter-rotating vortices. The instability apparently saturates shortly downstream from the exit, and the growth rate of the jet slows. The addition of swirl significantly alters the near-field development of the N-08 flow. Although the development of counter-rotating vortex pairs can still be observed very near the exit, vortices with the same sense of rotation (co-rotating) as the swirl rapidly diminished downstream. The process results in a flow that consists of a swirling main jet surrounded by eight vortices with the opposite sense of rotation (counter-rotating). The vortices follow stationary, spiraling paths around the main swirling jet. With or without swirl the jet shear layer begins to transition to turbulence at one to two diameters downstream from the exit. During the process, the outer vortices are integrated into the jet and can no longer be distinguished from the overall turbulence.

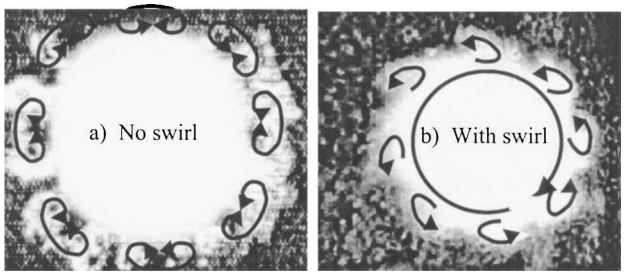

Fig. 3 Cross-sectional images of the N-08 jet with and without swirl; laser sheet is positioned normal to the jet axis at z/D of about 0.5.

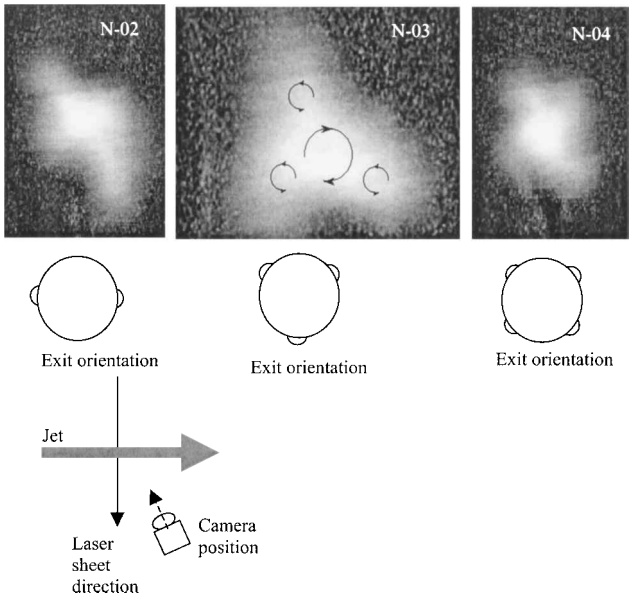

Fig. 4 Cross sections of the N-02, N-03, and N-04 jets with swirl. Images captured with the camera at an oblique angle to the laser sheet.

Cross sections of the N-02, N-03, and N-04 jets at about four diameters downstream from the exit are shown in Fig. 4. The initial developments of the N-04, N-03, and N-02 jets are qualitatively similar to the N-08. Shortly downstream from the exit, the addition of swirl results in the development of counter-rotating vortices around the main swirling jet. The number of perturbations (and thus vortices), however, has a stronger effect on the subsequent jet development than for the N-08 case.

Specifically, in comparison with N-08 jet, the effect of swirling on the N-04 jet is more pronounced and longer lasting. A four-lobed structure, similar to that produced by Wicker and Eatoin[5] using four large vortex generators mounted inside a nozzle, can be seen to develop and remains visible up to four diameters downstream from the exit. Beyond five diameters the jet development becomes similar to the N-08 jet. With no swirl the N-03 jet cross section takes on the somewhat triangular appearance. This is similar to the jet structure produced by Davis and Glezer[4] using three groups of synthetic jets for forcing. The addition of swirl significantly alters the flow. In this case a distinct three-lobed structure can be seen to develop shortly downstream from the exit and is still readily visible at $z/D = 10$. In the absence of swirl, the N-02 jet cross section takes on an elongated appearance that is visible far downstream of the exit. Even though the flow cross section is visually different from the N-08 jet, there does not appear to be a large difference in the overall growth rates. The addition of swirl, however, significantly changes the flow. A distinct two-lobed structure can be seen to develop. The flow structure persists for a long distance and is clearly visible at $z/D = 10$.

IV. Conclusions

The results can be summarized as follows:

1) For a jet with no swirl, pairs of counter-rotating, streamwise vortex structures are induced by discrete perturbations around the

exit circumference. The number of vortex pairs corresponds with the number of perturbations.

2) The combination of discrete perturbations along the exit circumference and swirling results in a flow structure that consists of a central swirling jet surrounded by vortices with the opposite sense of rotation. The number of outer vortices again corresponds with the number of perturbations.

3) For swirling jets with four or more perturbations, the effect is confined to a few diameters downstream from the exit.

4) The swirling jet with three perturbations develops a stable, three-lobed structure that persists farther than 10 diameters downstream from the exit.

5) The swirling jet with two perturbations develops a stable, two-lobed structure that persists farther than 10 diameters from the exit.

References

[1]Pierrehumber, R. T., and Widnall, S. E., "The Two- and Three-Dimensional Instabilities of a Spatially Periodic Shear Layer," *Journal of Fluid Mechanics*, Vol. 114, 1982, pp. 59–82.

[2]Long, T. A., and Petersen, R. A., "Controlled Interactions in a Forced Axisymmetric Jet. Part 1. The Distortion of the Mean Flow," *Journal of Fluid Mechanics*, Vol. 235, 1992, pp. 37–55.

[3]Longmire, E. K., Eaton, J. K., and Elkins, C. J., "Control of Jet Structure by Crown-Shaped Nozzles," *AIAA Journal*, Vol. 30, No. 2, 1992, pp. 505–512.

[4]Davis, S. A., and Glezer, A., "Mixing Control of Fuel Jets Using Synthetic Jet Technology: Velocity Field Measurements," AIAA Paper 99-0447, Jan. 1999.

[5]Wicker, R. B., and Eaton, J. K., "Effect of Injected Longitudinal Vorticity on Particle Dispersion in a Swirling, Coaxial Jet," *Journal of Fluid Engineering*, Vol. 121, Dec. 1999, pp. 766–772.

J. C. Hermanson
Associate Editor

Natural Frequencies of Cross-Ply Laminated Panels with Matrix Cracks

Victor Birman*
University of Missouri–Rolla, St. Louis, Missouri 63121
and
Larry W. Byrd†
U.S. Air Force Research Laboratory,
Wright–Patterson Air Force Base, Ohio 45433-7402

Introduction

MATRIX cracks appear in transverse layers of cross-ply laminates subjected to a relatively low tension. These cracks, called tunneling cracks, are perpendicular to the direction of the tensile load and parallel to the general fiber direction in the corresponding layer. Usually these cracks almost instantaneously propagate throughout the thickness of the layer and form a system of regularly spaced cracks. Such cracks were observed both in polymeric composites[1,2] as well as in ceramic matrix composites.[3,4] A number of theoretical models of the behavior of cross-ply laminates with matrix cracks in transverse layers have been developed. Most of these studies have been listed in a recent paper.[5] Han and Hahn expanded the analysis to the case where tunneling cracks exist in both transverse and longitudinal layers.[6]

Cross-ply laminates with matrix cracks behave in a manner similar to bimodular materials as a result of a different stiffness that depends on the cracks being open or closed. Therefore, the response in tension and in compression differs, although the borderline between the different responses depends on the exact value of the crack closing strain. This complication of the analysis makes it necessary to recall extensive work on mechanics of bimodular materials. Although a comprehensive review is outside the scope of this Note, mentioned here are the papers of Bert et al.,[7] Rebello et al.,[8] and Gordaninejad.[9]

The present Note outlines the analysis of free vibrations of a cross-ply plate with tunneling matrix cracks in all layers. The closed-form analytical solution is obtained in the paper utilizing the assumption that the cracks are closed under compression and the expressions for the engineering constants of cross-ply laminates with matrix cracks suggested by Han and Hahn.[6] The changes in natural frequencies considered in this Note are caused by a reduction of the stiffness. The effect of damping, which increases with cracking, is not accounted for in the present solution.

Analysis

Consider free vibrations of a thin cross-ply laminated plate with tunneling matrix cracks in the longitudinal and transverse layers (hereafter, longitudinal layers are oriented in the x direction and transverse layers are in the y direction). The plate can be asymmetrically laminated and the distribution of matrix cracks (crack density) can vary from layer to layer, although it is assumed here that this distribution is independent of the in-plane coordinates.

The analysis is based on the following assumptions:

1) The stiffness of a layer in the fiber direction is not affected by tunneling cracks. This reflects the observation that the planes of the cracks are parallel to the fibers of the corresponding layer and the fiber stiffness is the major contributor to the longitudinal stiffness.

2) Cracks are assumed to close under compression. Note that a crack closing strain may be estimated using the ratio of the crack opening displacement to the crack spacing (the latter is defined as a distance between the planes of parallel cracks). However, tunneling cracks reach saturation at the spacing, which is larger than the layer thickness, as was shown for both polymeric and ceramic matrix composites.[10,11] Therefore, the error introduced by the assumption that cracks close under compression cannot be large.

Although the longitudinal modulus of elasticity and the Poisson ratios of a compressed layer with closed cracks are recovered, the in-plane shear modulus depends on friction between the faces of closed cracks that has not been reported, to the best knowledge of the authors. If the friction coefficient is assumed negligible, the shear modulus is unaffected by the cracks being open or closed.

Small-amplitude free vibrations of the panel are analyzed by assumption that they do not result in additional damage. Accordingly, we consider the motion with preexisting matrix cracks, in which case thermal residual stresses do not affect the stiffness.[6] The expressions for engineering constants utilized in the subsequent calculations are based on the solution of Han and Hahn.[6] Based on these engineering constants, one can formulate the matrices of transformed reduced stiffnesses, as discussed next. For convenience, let us denote $z_1 = \max(z_x, z_y)$ and $z_2 = \min(z_x, z_y)$, where z_x and z_y are the locations of the neutral planes corresponding to zero axial strains ε_x and ε_y, respectively. It is assumed that during the part of the motion cycle considered next the cracks are open in all layers of the section of the laminate located within $z_1 < z < h/2$, whereas in the part corresponding to $-h/2 < z < z_2$ the cracks in both longitudinal and transverse layers are closed.

Matrix of Reduced Stiffnesses Within $z_1 < z < h/2$

The cracks are open in both longitudinal and transverse layers. Therefore, reduced stiffnesses Q'_{11}, Q'_{12}, Q'_{22}, and Q'_{66} can be determined in terms of the engineering constants E'_x, ν'_{xy}, E'_y, and G'_{xy} calculated according to the theory of Han and Hahn.[6] The engineering constants referred to in this Note are the average values for the material, rather than the constants for an individual layer. Notably, these constants depend on the density of cracks in several adjacent layers. Accordingly, they may vary throughout the depth of the panel, as is the case if matrix cracks were caused by bending.

Matrix of Reduced Stiffnesses Within $z_2 < z < z_1$

In this interval the cracks are closed in either longitudinal or transverse layers, whereas the cracks in the perpendicular layers are

Received 9 August 2000; revision received 25 September 2000; accepted for publication 27 September 2000.

*Professor and Director, Engineering Education Center, 8001 Natural Bridge Road. Associate Fellow AIAA.

†Engineer. Member AIAA.